

# 1           **Unveiling two new trichome-specific promoters of *Nicotiana tabacum***

2  
3   *Mathieu Pottier*<sup>§</sup>, *Raphaëlle Laterre*, *Astrid Van Wessem*, *Aldana M. Ramirez*, *Xavier*  
4   *Herman*, *Marc Boutry* and *Charles Hachez*<sup>\*</sup>

5  
6   Louvain Institute of Biomolecular Science and Technology, University of Louvain, 1348  
7   Louvain-la-Neuve, Belgium

8  
9   <sup>§</sup> Current address: InBioS-PhytoSYSTEMS, Laboratory of Plant Physiology, University of  
10   Liège, B-4000, Liège, Belgium

11  
12   <sup>\*</sup> Corresponding author: Charles Hachez, [charles.hachez@uclouvain.be](mailto:charles.hachez@uclouvain.be), + 32 10 47 37 96

13  
14   **ORCID:**

15   Mathieu Pottier: 0000-0003-1551-4699

16   Marc Boutry: 0000-0002-2315-6900

17   Charles Hachez: 0000-0002-3688-7614

18  
19   **Author contributions** MP, RL, CH and MB designed the experiments and analyzed the data.  
20   MP, RL, AVW, AR, XH and MB performed experiments. CH, MP and MB wrote the  
21   manuscript.

22  
23   **Acknowledgments** The authors are grateful to Joseph Nader for his technical contribution.  
24   This work was supported by the Belgian Fund for Scientific Research (Grant ID: MIS –  
25   F.4522.17), the Interuniversity Poles of Attraction Program (Belgian State, Scientific,  
26   Technical and Cultural Services), and an EU Marie Skłodowska-Curie fellowship (Project ID:  
27   658932) to MP.

28  
29   **Conflict of Interest** The authors declare that they have no conflict of interest.

30 **Abstract**

31 **Main conclusion** *pRbcS-T1* and *pMALD1*, two new trichome-specific promoters of  
32 *Nicotiana tabacum*, were identified and their strength and specificity were compared to  
33 those of previously described promoters in this species.

34  
35 **Abstract** *Nicotiana tabacum* has emerged as a suitable host for metabolic engineering of  
36 terpenoids and derivatives in tall glandular trichomes, which actively synthesize and secrete  
37 specialized metabolites. However, implementation of an entire biosynthetic pathway in  
38 glandular trichomes requires the identification of trichome-specific promoters to appropriately  
39 drive the expression of the transgenes needed to set up the desired pathway. In this context,  
40 RT-qPCR analysis was carried out on wild-type *N. tabacum* plants to compare the expression  
41 pattern and gene expression level of *NtRbcS-T1* and *NtMALD1*, two newly identified genes  
42 expressed in glandular trichomes, with those of *NtCYP71D16*, *NtCBTS2 $\alpha$* , *NtCPS2*, and  
43 *NtLTPI*, which were reported in the literature to be specifically expressed in glandular  
44 trichomes. We show that *NtRbcS-T1* and *NtMALD1* are specifically expressed in glandular  
45 trichomes like *NtCYP71D16*, *NtCBTS2 $\alpha$* , and *NtCPS2*, while *NtLTPI* is also expressed in  
46 other leaf tissues as well as in the stem. Transcriptional fusions of each of the six promoters to  
47 the *GUS-VENUS* reporter gene were introduced in *N. tabacum* by *Agrobacterium*-mediated  
48 transformation. Almost all transgenic lines displayed GUS activity in tall glandular trichomes,  
49 indicating that the appropriate cis regulatory elements were included in the selected promoter  
50 regions. However, unlike for the other promoters, no trichome-specific line was obtained for  
51 *pNtLTPI:GUS-VENUS*, thus in agreement with the RT-qPCR data. These data thus provide  
52 two new transcription promoters that could be used in metabolic engineering of glandular  
53 trichomes.

54  
55 **Keywords** Rubisco small subunit, Major Allergen Mal D 1.0501, Cembratrien-ol Synthase,  
56 Copal-8-ol diphosphate Synthase, Lipid Transfer Protein, Cytochrome P450 oxygenase

## 57 **Introduction**

58 Trichomes are epidermal outgrowths covering most of aerial tissues in a large number of  
59 plant species. Several types of trichomes (unicellular or multicellular, glandular or non-  
60 glandular) can be observed in a single plant species. Among those, glandular trichomes are  
61 characterized by cells forming a glandular structure that secretes or stores specialized (also  
62 called secondary) metabolites (e.g., phenylpropanoids, flavonoids, acyl sugars,  
63 methylketones, and terpenoids). Many of these possess antimicrobial and antifungal  
64 properties or act as a defense barrier against herbivorous insects (Schilmiller et al. 2008).

65 The specialized metabolites secreted by glandular trichomes, which might represent up to  
66 17 % of the leaf dry weight in *Nicotiana tabacum* (tobacco), have been largely exploited over  
67 centuries (Wagner et al. 2004). One of their most ancient uses originates from their aromatic  
68 properties and fragrances. Besides, these specialized metabolites constitute an interesting  
69 source of pharmaceuticals and food additives. Some specialized metabolites are only found in  
70 a single plant species or even a single plant cultivar and often at low concentration (e.g., taxol  
71 found in *Taxus sp.*, artemisinin in *Artemisia annua* or cannabinoids in *Cannabis sativa*).  
72 Therefore, natural resources are often insufficient to reach the global need (Van Agtmael et al.  
73 1999; Yoon et al. 2013), while the complex stereochemistry of these compounds often  
74 prevents their full chemical synthesis in a cost-effective way.

75 In order to increase the overall yield, metabolic engineering strategies are undertaken in a  
76 variety of host species (Kirby and Keasling 2009; Marienhagen and Bott 2013). Advances in  
77 plant biotechnology and increasing knowledge in specialized metabolism also make possible  
78 to exploit plants as production platforms. One of the main advantages of using them is that  
79 they are photoautotrophic organisms, therefore requiring simple and cheap growth conditions,  
80 which accounts for a cost-effective production (Kempinski et al. 2015). In addition, their  
81 ability to deal with membrane proteins such as P450 enzymes and posttranslational  
82 modifications such as glycosylation, are two key features frequently limiting in prokaryotic  
83 hosts (van Herpen et al. 2010).

84 Terpenoids and derivatives are the most abundant plant specialized metabolites in terms of  
85 sheer number and chemical diversity (for review, see Croteau et al. 2000; Bouvier et al. 2005;  
86 Gershenzon and Dudareva 2007) and *N. tabacum* has emerged as one of the most suitable  
87 plant hosts for their biosynthesis (Moses and Pollier 2013; Lange et al. 2013; Wang et al.  
88 2016). Indeed, *N. tabacum* synthesizes a very high amount of a limited range of specialized  
89 metabolites (Huchelmann et al. 2017). This combined to its high biomass, its fast growth rate,

90 and its easy genetic transformation make it an interesting host to implement the biosynthesis  
91 pathways of terpenoid compounds and derivatives thereof.

92 However, engineering terpenoid biosynthetic pathways using ubiquitous promoters  
93 frequently leads to severe phenotypes including dwarfism, chlorosis, and decreased seed  
94 production due to the cytotoxicity of these compounds or detrimental impact on the  
95 biosynthesis of essential metabolites (Saxena et al. 2014; Gwak et al. 2017; reviewed in  
96 Huchelmann et al. 2017). To avoid these adverse effects, a fine control of the spatiotemporal  
97 expression of the transgenes, restricting the biosynthesis of potentially cytotoxic metabolites  
98 to specialized organs, is desirable (Huchelmann et al. 2017). Since *N. tabacum* glandular  
99 trichomes contain an important pool of terpenoid precursors and have naturally evolved to  
100 deal with high concentrations of terpenoids, they make ideal targets to develop such a  
101 metabolic engineering approach. For this purpose, identification of trichome-specific  
102 transcription promoters is required.

103 A proteomic comparison was recently performed in *N. tabacum* between proteins  
104 extracted from tall glandular trichomes and those extracted from other plant organs (Laterre et  
105 al. 2017). This led to the identification of 47 proteins that were more abundant in tall  
106 glandular trichomes, the most enriched ones being a putative PR-10 type pathogenesis-related  
107 protein, namely Major Allergen Mal D 1.0501 (MALD1) and a Ribulose-1,5-Bisphosphate  
108 Carboxylase/oxygenase Small subunit (RbcS-T1) (Laterre et al. 2017). For both, semi-  
109 quantitative RT-PCR supports trichome-specific localization of their corresponding  
110 transcripts (Harada et al. 2010; Laterre et al. 2017).

111 This suggests that *the NtMALD1* and *NtRbcS-T* promoters may confer trichome-specificity,  
112 as those of CYtochrome P450 oxygenase 71D16 (*NtCYP71D16*), Copal-8-ol diPhosphate  
113 Synthase 2 (*NtCPS2*), Lipid Transfer Protein 1 (*NtLTPI*), and CemBraTrien-ol Synthase 2 $\alpha$   
114 (*NsCBTS2 $\alpha$* ) previously described (Wang et al. 2002; Ennajdaoui et al. 2010; Choi et al. 2012;  
115 Sallaud et al. 2012). However, these six genes were investigated separately, preventing one to  
116 compare their transcript levels. In addition, for some of them, cell-type specificity monitored  
117 by the GUS reporter gene was not described in other organs than leaves. The present study  
118 thus aimed at comparing the expression patterns and expression levels of *NtCYP71D16*,  
119 *NtCBTS2 $\alpha$* , *NtCPS2*, *NtLTPI*, *NtRbcS-T1*, and *NtMALD1* in *N. tabacum*. Their transcript levels  
120 in trichomes and different organs were compared. Transcriptional fusions of each promoter to  
121 *GUS-VENUS* were expressed in transgenic *N. tabacum* plants. GUS staining corroborate

122 transcripts data and indicate that all promoters, except for *pNtLTP1*, can be used to drive  
123 trichome-specific expression.

124

## 125 **Materials and methods**

### 126 **Plant material and plant growth conditions**

127 *Nicotiana tabacum* cv Petit Havana SR1 (Maliga et al. 1973) plants were used in this work.  
128 For the *in vitro* cultures, seeds were sterilized by immersion in 1 ml 70% (v/v) ethanol for 1  
129 min and then in 1 ml 50% (v/v) commercial bleach for 2 min. Seeds were then washed three  
130 times with 1 ml of sterile MilliQ water and kept at 4°C, in the dark, during 48 h for  
131 stratification. Sterilized seeds were sown on solid Murashige and Skoog (MS) medium [4.33  
132 g.l<sup>-1</sup> MS salts (MP Biochemicals, Solon, OH, USA; www.mpbio.com), 3% (w/v) sucrose, 1%  
133 (w/v) agar, pH 5.8 (KOH)] and placed in the growth chamber at 25°C under a 16 h  
134 photoperiod (50 μmol photon m<sup>-2</sup> sec<sup>-1</sup>). For the soil cultures, seeds were stratified before  
135 being sown in potting soil (DCM, Grobbendonk, Belgium; dcm-info.com). Isolated plantlets  
136 coming from potting soil or *in vitro* conditions were transferred to Jiffy pots (Gronud,  
137 Norway; www.jiffypot.com) before being transferred to bigger pots containing potting soil  
138 (DCM). Plants on soil were grown under controlled conditions, in a phytotron set at 25°C and  
139 with a 16 h photoperiod (300 μmol photon m<sup>-2</sup> sec<sup>-1</sup>).

140

### 141 **Tissue isolation, RNA extraction and cDNA synthesis**

142 Trichomes were removed from tissues of 6-week-old plants following the cold-brushing  
143 method (Wang et al. 2001). For gene expression in trichomes during leaf development, the  
144 analysis was performed in triplicate. Trichomes were isolated from leaves at different  
145 developmental stages defined here by leaf length: < 2.5 cm (stage I), between 2.5 cm and 6.5  
146 cm (stage II), between 6.5 cm and 15 cm (stage III), and > 15 cm (stage IV). For gene  
147 expression in different tissues, the analysis was performed in three to five replicates on roots,  
148 trichomes-free stems, trichomes-free leaves, and leaf trichomes (pool of leaves from stage I to  
149 stage III) from 6-week-old plants, and flowers from 10-week-old plants. For each biological  
150 replicate (except for isolated trichomes), 100 mg of material was pre-ground in liquid nitrogen  
151 using a mortar and pestle. Pre-ground tissues and isolated trichomes were ground in 2 mL  
152 Precellys tubes containing 200 μl of ceramic beads Zirmil (0.5 mm, Saint Gobain Zipro, Le  
153 Pontet, France) and 500 μl of lysis/2-Mercaptoethanol solution of the Spectrum<sup>TM</sup> Plant Total  
154 RNA Kit (Sigma-Aldrich, St. Louis, Missouri, USA; <http://www.sigmaaldrich.com>). Samples

155 were subjected to four consecutive 30 s grinding periods at 6,000 rpm using a Precellys 24  
156 (Bertin Technologies, Montigny-le-Bretonneux, France). The homogenates were centrifuged  
157 at 1,000 g for 3 min (Eppendorf 5430, Hamburg, Germany). The subsequent steps of the RNA  
158 extraction were performed on the supernatants according to the manufacturer's specifications,  
159 except that the 56 °C incubation step was omitted. RNA was eluted in 50 µl elution buffer and  
160 quantified using a spectrophotometer (Nanodrop® ND-1000, Isogen Life Science, The  
161 Netherlands; www.isogen-lifescience.com). Genomic DNA contamination was eliminated by  
162 using the On-Column DNase I Digestion Set (Sigma-Aldrich, St. Louis, Missouri, USA;  
163 www.sigmaaldrich.com). The RNA was finally flash frozen in liquid nitrogen and stored at -  
164 80°C. DNA-free RNA (500 µg) was used for reverse transcription using the Moloney Murine  
165 Leukemia Virus Reverse transcriptase (Promega, Madison, Wisconsin, USA;  
166 be.promega.com) and oligo(dT)<sub>18</sub>. Reverse transcription mixture was added according to the  
167 manufacturer's specifications. After adding the transcriptase, samples were incubated for 5  
168 min at 25°C, followed by 1 h at 42°C and 5 min at 85°C, placed on ice for 5 min, aliquoted,  
169 and stored at -20°C.

170

### 171 **Gene expression**

172 Gene-specific RT-qPCR primers listed in Supplemental Table S1 were designed at the  
173 3' end of the coding sequence, (size, about 100 bp; melting temperature, 60°C) using  
174 OligoPerfect™ Designer (www.thermofisher.com). cDNA (5 µl, 17 fold diluted) was used as  
175 a template in 20 µl RT-qPCR reaction, which also contained 10 µl of the Power SYBR green  
176 PCR master mix of qPCR master mix plus for SYBR Green I (Eurogentec, Seraing, Belgium,  
177 <https://secure.eurogentec.com/eu-home.html> ) and 5 µl of primer mix (1.3 µM each).  
178 Amplification was performed on an ABI 7500 Real-Time PCR system (Waltham,  
179 Massachusetts, USA; <http://www.thermofisher.com>). Primer specificity was confirmed by  
180 analysis of the melting curves. For each tissue, primer amplification efficiency ( $\geq 95\%$ ) was  
181 determined using five standards from serial dilutions of a cDNA pool of the biological  
182 replicates used for gene expression analysis. Relative transcript levels were calculated  
183 following the  $2^{-\Delta\Delta C_t}$  method (Livak and Schmittgen 2001) with the geometric mean of  
184 mitochondrial ATP-synthase  $\beta$ -subunit (*NtATP2*), ubiquitin (*NtUBQ*), and elongation factor  $\alpha$   
185 (*NtEF1 $\alpha$* ) transcripts used as reference for comparison between different tissues (three to five  
186 replicates), and of *NtATP2*, *NtUBQ*, and actin (*NtACTIN*), for comparison between different  
187 leaf developmental stages (three replicates). For absolute quantification (three replicates),  
188 PCR products amplified by gene-specific RT-qPCR primers listed in Supplemental Table S1

189 were cloned in pGEM-T Easy vector (Promega, Madison, Wisconsin, USA) prior to their  
190 sequencing. Constructs were linearized by *PstI* restriction, purified using Nucleospin Extract  
191 II kit (Macherey-Nagel, Düren, Germany) and rigorously quantified through UV (260 nm)  
192 absorption using a spectrophotometer (Nanodrop® ND-1000, Isogen Life Science, The  
193 Netherlands; www.isogen-lifescience.com). For each quantified purified linear plasmid, the  
194 copy number was determined according to the following equation (Godornes et al. 2007):  
195 copy number = (vector amount [g]) × 6.023 × 10<sup>23</sup> [molecules/mole] / (660 [g/mole/base] ×  
196 size of the vector+insert [bases]). Absolute transcript levels were then determined through the  
197 absolute standard curve method. Thus, for each studied gene, standards (2 × 10<sup>6</sup>, 2 × 10<sup>5</sup>, 2 ×  
198 10<sup>4</sup>, 2 × 10<sup>3</sup> copies) obtained by serial dilution of the purified linear plasmids were included in  
199 duplicate in q-PCR plates used to study gene expression during trichome development.

200

### 201 **Generation of plants expressing *PROMOTER:GUS-VENUS* fusions**

202 The transcription promoter regions of *NtRbcS-T1* (1993 pb; GenBank accession:  
203 MG493459.1) and *NtMALDI* (1974 pb; GenBank accession: MG493458.1) were identified  
204 blasting the EST corresponding to *NtRbcS-T1* (GenBank accession: DV157962) and  
205 *NtMALDI* (GenBank accession: FS387666) coding sequences to the genome of *N.*  
206 *tabacum* TN90 in the Solgenomics database (<http://solgenomics.net>). The promoter regions of  
207 *NsCBTS2α* (985 bp; GenBank accession: HM241151.1), *NtLTP1* (849 bp; GenBank  
208 accession: AB625593.1), *NtCYP71D16* (1852 pb; GenBank accession: AF166332.1), and  
209 *NtCPS2* (1448 bp; GenBank accession: HE588139.1) were defined as previously (Wang et al.  
210 2002; Ennajdaoui et al. 2010; Choi et al. 2012; Sallaud et al. 2012). Promoter regions were  
211 amplified by PCR using as a template genomic DNA prepared from *N. tabacum* or *N.*  
212 *sylvestris* leaves and the primers listed in Supplemental Table S2. The amplified fragments  
213 were inserted in the pGEM®-T Easy Vector (Promega, Madison, Wisconsin, USA;  
214 www.promega.com) and sequenced. Cloned fragments were cleaved using *HindIII* (or *NotI*  
215 for *pNtMALDI* and *pNtRbcS-T1*) and *KpnI*, prior to their insertion in a pAUX3131 construct  
216 (Navarre et al. 2011), upstream of the *GUS-VENUS* coding sequence. The fusion construct  
217 was excised using *I-SceI* and inserted into the pPZP-RCS2-nptII plant expression vector  
218 (Goderis et al. 2002), also cut with *I-SceI*. The construct was introduced into *Agrobacterium*  
219 *tumefaciens* LBA4404 virGN54D (van der Fits et al. 2000) for subsequent *N. tabacum* leaf  
220 disc transformation (Horsch et al. 1986). For each construct, 24 to 45 independent transgenic  
221 lines were generated and finally transferred to soil to be analyzed by GUS staining.

222

## 223 **GUS histochemical analysis**

224 Histochemical staining of plant tissues for GUS activity was conducted during 3h30 as  
225 described previously (Bienert et al. 2012). However, to allow substrate access to the  
226 trichomes covered by the oily exudate, incubation was performed in the presence of 1%  
227 Triton X-100.

228

## 229 **Statistical analysis**

230 All tests were performed using the R software. For q-PCR, data were analyzed using  
231 *kruskal.test* (Kruskal–Wallis) function for multiple comparisons. For multiple comparisons,  
232 *npaircomp* package was used to perform Tukey post-hoc test when significant differences  
233 were detected ( $P < 0.05$ ). Different letters indicate significant differences between samples.

234

## 235 **Results**

236

237 In a 2D gel analysis of glandular trichome proteins from *N. tabacum*, several spots were  
238 identified as trichome-specific proteins, among which RbcS-T1 and MALD1 (Laterre et al.  
239 2017). Here, the RNA levels of *NtRbcS-T1* and *NtMALD1* as well as of *NtLTPI*, *NtCYP71D16*,  
240 *NtCBTS2 $\alpha$* , and *NtCPS2* previously reported as genes specifically expressed in tall glandular  
241 trichomes, were compared in trichomes and different *N. tabacum* organs. To do so, leaves  
242 were frozen in liquid nitrogen and carefully scratched with a brush to collect the trichomes.  
243 RT-qPCR assays were then performed on RNA extracted from trichomes, roots, trichome-free  
244 leaves, and trichome-free stems of six-week-old plants as well as from flowers of 10-week-  
245 old plants. Unlike for leaves and stems, trichomes could not be retrieved from flower sepals  
246 and petals. Because different organs had to be compared, it was important to use reference  
247 genes, whose expression little varies according to the organ. The transcript levels of ubiquitin  
248 (*NtUBQ*), mitochondrial ATP-synthase  $\beta$ -subunit (*NtATP2*), actin (*NtACTIN*), and elongation  
249 factor  $\alpha$  (*NtEF1 $\alpha$* ), frequently described as reference genes, were thus monitored. On the basis  
250 of this analysis, we found that *NtUBQ*, *NtATP2*, and *NtEF1 $\alpha$*  genes were the most stable,  
251 therefore the geometric mean of their transcripts was used to normalize the data  
252 (Supplemental Fig. S1). For each studied gene, the relative expression level in trichomes was  
253 arbitrarily set to one. All six investigated genes showed a higher relative expression level in  
254 isolated trichomes compared to the levels observed in roots, leaves, stems or flowers (Fig. 1).  
255 *NtCYP71D16*, *NtCBTS2 $\alpha$* , *NtCPS2*, *NtRbcS-T1*, and *NtMALD1* exhibited very low or even  
256 undetectable expression in roots, trichome-free leaves and trichome-free stems, while higher



257 transcript levels were found for *NtLTP1* in leaves and stems. Expression was observed in  
258 flowers for the six genes but, as noted above, sepal and petal trichomes could not be removed  
259 from these organs.

260 As most of these genes are involved in the biosynthesis (*NtCYP71D16*, *NtCBTS2 $\alpha$* , and  
261 *NtCPS2*) or transport (*NtLTP1*) of specialized metabolites secreted by mature glands, we  
262 wondered whether the leaf developmental stage could impact their expression in trichomes.  
263 Thus, glandular trichomes were isolated from leaves at different developmental stages,  
264 arbitrarily defined by the leaf length: < 2.5 cm (stage I), between 2.5 cm and 6.5 cm (stage II),  
265 between 6.5 cm and 15 cm (stage III), and > 15 cm (stage IV). In this experiment, *NtUBQ*,  
266 *NtATP2*, and *NtACTIN* transcripts were the most stable, therefore the geometric mean of their  
267 transcripts was used to normalize the data (Supplemental Fig. S2). While the transcript level  
268 of *NtLTP1* appeared stable during leaf development, expression of the other five genes  
269 steadily increased until stage III where it reached a plateau (Fig. 2). The opposite trend was  
270 observed for elongation factor  $\alpha$  (*NtEF1 $\alpha$* ), which peaked at stage I (Supplemental Fig. S2),  
271 confirming that the observed increasing level of these five genes is not an artifact of the  
272 normalization method. Among them, *NtRbcS-T1* was the gene for which the transcript level  
273 increased the most with leaf development (4-fold increase). Expression of *NtCBTS2 $\alpha$*  and  
274 *NtCYP71D16* involved in the biosynthesis of cembrenes, the major subgroup of diterpenes  
275 produced by *N. tabacum* glandular trichomes, also exhibited a large increase (3.8- and 3.6-  
276 fold, respectively) (Fig. 2). A more moderate increase was found for *NtMALD1* (2.6-fold) and  
277 *NtCPS2* (2.4-fold) transcripts, the latter being involved in the biosynthesis of another  
278 subgroup of diterpenes, namely labdanes.

279 The absolute expression levels of all six genes of interest was then determined using the  
280 absolute standard curve method in isolated trichomes for developmental stage III at which all  
281 genes reached a maximal expression, (Fig. 3, see Material and methods for details). Several  
282 control genes, some of which were used to normalize the relative expression data shown in  
283 Figures 1 and 2, were also added to the study for comparison purposes. Among control genes,  
284 the absolute expression levels (Fig. 3) were in agreement with previously published data in  
285 other Solanaceae species (Lu et al. 2012; Lacerda et al. 2015). Genes involved in cembrene  
286 production, *NtCBTS2 $\alpha$*  (78.0 copies/pg), and *NtCYP71D16* (67.9 copies/pg), were the most  
287 expressed genes at stage III (Fig. 3), while a lower expression was found at this stage for  
288 *NtMALD1* (40.8 copies/pg), *NtLTP1* (28.2 copies/pg), *NtCPS2* (labdane diterpenes, 11.1  
289 copies/pg) and *NtRbcS-T1* (5.1 copies/pg).

290 To further confirm the trichome-specific expression pattern observed by RT-qPCR, we  
291 generated transcriptional reporter lines using a *GUS-VENUS* coding sequence. In the 2D gel  
292 analysis which led to the identification of trichome-specific proteins, two spots had been  
293 identified as trichome-specific RbcS (Laterre et al. 2017). At that time, only the *N.*  
294 *benthamiana* genome sequence was available and a RbcS transcription promoter (*pNbrbcS-*  
295 *T*) corresponding to the minor RbcS spot had been retrieved from this species and  
296 characterized (Laterre et al. 2017). Once the sequence of a *N. tabacum* genome became  
297 available, we identified *pNtrbcS-T1* (accession: MG493459.1) as the promoter of the gene  
298 corresponding to the major trichome RbcS spot (NtrbcS-T1; accession: DV157962). The  
299 *NtMALD1* promoter (accession: MG493458.1), corresponding to the NtMALD1 spot  
300 (accession: FS387666) was identified as well. The *GUS-VENUS* coding sequence was fused  
301 to *N. tabacum* genomic fragments of 1993 bp and 1974 bp upstream of the translation  
302 initiation codon of *NtrbcS-T1* and *NtMALD1*, respectively (Fig. 4). For the other genes, the  
303 previously published promoter regions, i.e. 985 bp (*NsCBTS2a*), 849 bp (*NtLTP1*), 1852 bp  
304 (*NtCYP71D16*), and 1448 bp (*NtCPS2*) (Wang et al. 2002; Ennajdaoui et al. 2010; Choi et al.  
305 2012; Sallaud et al. 2012) were isolated and similarly fused to the *GUS-VENUS* coding  
306 sequence. These constructs were introduced in *N. tabacum* through *Agrobacterium*  
307 *tumefaciens*-mediated transformation. For each construct, 24 to 45 independent transgenic  
308 lines were generated and their GUS activity was monitored in T<sub>0</sub> and then confirmed on T<sub>1</sub>  
309 lines. A large majority (83-95%) of the generated lines displayed GUS activity in tall  
310 glandular trichomes. This indicates that appropriate cis-sequences required for expression in  
311 tall glandular trichomes are present in the promoter sequences fused to the reporter gene. With  
312 the exception of the *pNtLTP1:GUS-VENUS* reporter (see below), several lines for the other  
313 constructs had their GUS activity restricted to glandular trichomes on aerial parts of the plant  
314 (examples are displayed for each construct in Fig. 5a-r and Supplemental Fig. 3) while no  
315 signal was recorded in roots (Supplemental Fig. 3). In these lines, trichome expression was  
316 further confirmed by following VENUS fluorescence on living tissue by confocal microscopy  
317 (Fig. 5). The *NtCPS2* promoter provided strong expression in both leaf short and tall  
318 glandular trichomes, while the other four constructs only labelled tall glandular trichomes  
319 (Fig. 5j-l).

320 For each of these five constructs, other lines had their expression extended to other cell  
321 types, with a pattern and an intensity varying according to the line, a typical consequence of  
322 the position effect (see discussion). As an exception, all *pNtLTP1:GUS-VENUS* lines

323 displayed GUS activity in various leaf and stem tissues (Fig. 5p-r and Supplemental Fig. 3),  
324 confirming the absence of trichome specificity revealed by RT-qPCR data.

325

## 326 **Discussion**

327

328 In this work, the tissue-specific expression pattern of six *N. tabacum* genes, namely  
329 *NtLTP1*, *NtCYP71D16*, *NtCBTS2 $\alpha$* , *NtCPS2*, *NtRbcS-T1*, and *NtMALD1*, was analyzed. In  
330 fact, although these genes were previously described as trichome-specific, their trichome-  
331 specific expression at the transcript level had not yet been quantified and compared. We  
332 performed this comparison through RT-qPCR using RNA isolated from trichomes and  
333 different plant organs as well as *GUS-VENUS* reporter genes using, when available,  
334 previously published promoter sequences.

335 RT-qPCR analysis showed that all these genes except for *NtLTP1*, are specifically  
336 expressed in trichomes in *N. tabacum* (Fig. 1). Regarding *NtLTP1* transcripts, they were also  
337 identified in leaf and stem tissues cleared from trichomes (Fig. 1). This observation is in line  
338 with previously published semi-quantitative RT-PCR which showed that *NtLTP1* is expressed  
339 in different organs (Fig. 1; Harada et al., 2010). Apart from *NtLTP1*, whose expression was  
340 almost constant during leaf development, that of the other five genes was lower at an early  
341 stage of leaf development and reached a maximum at stage III (Fig. 2), presumably when the  
342 specialized metabolism in which they are involved is fully operating. This is also true for  
343 *NtRbcS-T1* and this observation is in agreement with the hypothesis that in glandular  
344 trichomes, Rubisco recycles the CO<sub>2</sub> released by the specialized metabolism (Pottier et al.  
345 2018). These expression data may help choose appropriate trichome-specific promoters to  
346 drive the expression of a transgene for metabolic engineering purposes. Although  
347 *NtCYP71D16* and *NtCBTS2 $\alpha$*  lead to higher expression level in trichomes at stage III of leaf  
348 development, *NtCPS2* and *NtMALD1* promoters should lead to a more homogenous  
349 expression of transgenes among leaves at different developmental stages.

350 Our analysis of *GUS-VENUS* reporter lines revealed that, in almost all of them, the six  
351 promoters drove gene expression in the head cells of tall glandular trichomes of *N. tabacum*  
352 (Fig. 5). However, in agreement with the transcript level analysis (Fig. 1; Harada et al., 2010),  
353 we observed GUS reporter activity in other organs than trichomes in all the lines expressing  
354 the *NtLTP1:GUS-VENUS* construct (Fig. 5p-r and Supplemental Fig. S4p-r). The examination  
355 of similar lines by Choi et al., (2012) has also revealed some GUS reporter activity in other  
356 cell types than trichomes while the expression in the stem was not displayed. We thus

357 conclude that the *NtLTPI* promoter does not confer trichome-specific expression. On the  
358 contrary, trichome-specific GUS activity was observed in lines expressing any of the five  
359 other constructs (Fig. 5 and Supplemental Fig. S4), which is consistent with our RT-qPCR  
360 analysis (Fig. 1). However, other lines displayed GUS expression in trichomes, but also in  
361 other cell types, with a profile varying from line to line for a given reporter construct (data not  
362 shown). This likely results from a position effect due to the random insertion of the T-DNA in  
363 the plant cell genome. The genomic environment surrounding the integrated cassette  
364 (structure of chromatin, presence of enhancers/silencers near the insertion site) is known to  
365 alter the expression level and profile of transgenes (Kohli et al. 2010; Hernandez-Garcia and  
366 Finer 2014). Between independent lines, and thus different insertion sites, this position effect  
367 differs according to the proximal endogenous regulatory elements.

368 In conclusion, a key and unique feature of glandular trichomes is their ability to synthesize  
369 and secrete large amounts of a limited panel of specialized metabolites. Taking advantage of  
370 the pool of natural precursors to produce specific metabolites in glandular trichomes by  
371 metabolic engineering would therefore be of high biotechnological interest. This requires the  
372 availability of transcriptional promoters specifically active in these structures that could be  
373 used to efficiently drive the expression of the transgenes coding for the enzymes needed to  
374 implement the pathway in a cell-type specific way. In this respect, the identification of the  
375 *NtMALDI* and *NtRbS-T1* promoters and their comparison with previously identified trichome-  
376 specific promoters are promising tools for expressing entire biosynthesis pathways in  
377 glandular trichomes of *N. tabacum*.

378

379

380 **Supplementary data**

381 **Supplemental Fig. 1** Transcript levels of control genes in different organs of *N. tabacum*

382 **Supplemental Fig. 2** Transcript levels of control genes in trichomes isolated from *N.*  
383 *tabacum* leaves at different developmental stages

384 **Supplemental Fig. 3** GUS activity in various tissues of *N. tabacum* transgenic lines.

385 **Supplemental Table S1** List of primers used for RT-qPCR.

386 **Supplemental Table S2** List of primers used to amplify the promoter sequences.

387

388 **References**

- 389 Bienert MD, Delannoy M, Navarre C, Boutry M (2012) NtSCP1 from Tobacco Is an  
390 Extracellular Serine Carboxypeptidase III That Has an Impact on Cell Elongation. *Plant*  
391 *Physiol* 158:1220–1229. <https://doi.org/10.1104/pp.111.192088>
- 392 Bouvier F, Rahier A, Camara B (2005) Biogenesis, molecular regulation and function of plant  
393 isoprenoids. *Prog Lipid Res* 44:357–429. <https://doi.org/10.1016/j.plipres.2005.09.003>
- 394 Choi YE, Lim S, Kim H-J, et al (2012) Tobacco NtLTP1, a glandular-specific lipid transfer  
395 protein, is required for lipid secretion from glandular trichomes. *Plant J* 70:480–91.  
396 <https://doi.org/10.1111/j.1365-313X.2011.04886.x>
- 397 Croteau R, Kutchan TM, Lewis NG (2000) Natural Products (Secondary Metabolites). In:  
398 Buchanan B, Gruissem W, Jones R (eds) *Biochemistry & Molecular Biology of Plants*.  
399 American Society of Plant Physiologists, pp 1250–1318
- 400 Ennajdaoui H, Vachon G, Giacalone C, et al (2010) Trichome specific expression of the  
401 tobacco (*Nicotiana glauca*) cembratrien-ol synthase genes is controlled by both  
402 activating and repressing cis-regions. *Plant Mol Biol* 73:673–85.  
403 <https://doi.org/10.1007/s11103-010-9648-x>
- 404 Gershenzon J, Dudareva N (2007) The function of terpene natural products in the natural  
405 world. *Nat Chem Biol* 3:408–414. <https://doi.org/10.1038/nchembio.2007.5>
- 406 Goderis IJWM, De Bolle MFC, François IEJA, et al (2002) A set of modular plant  
407 transformation vectors allowing flexible insertion of up to six expression units. *Plant*  
408 *Mol Biol* 50:17–27. <https://doi.org/10.1023/A:1016052416053>
- 409 Godornes C, Troy B, Molini BJ, et al (2007) Quantitation of rabbit cytokine mRNA by real-  
410 time RT-PCR. 38:1–7. <https://doi.org/10.1016/j.cyto.2007.04.002>
- 411 Gwak YS, Han JY, Adhikari PB, et al (2017) Heterologous production of a ginsenoside  
412 saponin (compound K) and its precursors in transgenic tobacco impairs the vegetative  
413 and reproductive growth. *Planta* 245:1105–1119. [https://doi.org/10.1007/s00425-017-](https://doi.org/10.1007/s00425-017-2668-x)  
414 [2668-x](https://doi.org/10.1007/s00425-017-2668-x)
- 415 Harada E, Kim J-AA, Meyer AJ, et al (2010) Expression profiling of tobacco leaf trichomes  
416 identifies genes for biotic and abiotic stresses. *Plant Cell Physiol* 51:1627–1637.  
417 <https://doi.org/10.1093/pcp/pcq118>
- 418 Hernandez-Garcia CM, Finer JJ (2014) Identification and validation of promoters and cis-  
419 acting regulatory elements. *Plant Sci* 217–218:109–119.  
420 <https://doi.org/10.1016/j.plantsci.2013.12.007>

421 Horsch RB, Klee HJ, Stachel S, et al (1986) Analysis of *Agrobacterium tumefaciens* virulence  
422 mutants in leaf discs. *Proc Natl Acad Sci U S A* 83:2571–2575.  
423 <https://doi.org/10.1073/pnas.83.8.2571>

424 Huchelmann A, Boutry M, Hachez C (2017) Plant glandular trichomes: natural cell factories  
425 of high biotechnological interest. *Plant Physiol* 175:6–22.  
426 <https://doi.org/10.1104/pp.17.00727>

427 Kempinski C, Jiang Z, Bell S, Chappell J (2015) Metabolic engineering of higher plants and  
428 algae for isoprenoid production. In: Schrader J, Bohlmann J (eds) *Biotechnology of*  
429 *Isoprenoids*. Springer International Publishing, Cham, pp 161–199

430 Kirby J, Keasling JD (2009) Biosynthesis of Plant Isoprenoids: Perspectives for Microbial  
431 Engineering. *Annu Rev Plant Biol* 60:335–55.  
432 <https://doi.org/10.1146/annurev.arplant.043008.091955>

433 Kohli A, Miro B, Twyman RM (2010) Chapter 7 Transgene Integration, Expression and  
434 Stability in Plants: Strategies for Improvements. In: C. Kole et al. (ed) *Transgenic Crop*  
435 *Plants*. Springer-Verlag, Berlin, Heidelberg, pp 201–237

436 Lacerda ALM, Fonseca LN, Blawid R, et al (2015) Reference gene selection for qPCR  
437 analysis in tomato-bipartite begomovirus interaction and validation in additional tomato-  
438 virus pathosystems. *PLoS One* 10:1–17. <https://doi.org/10.1371/journal.pone.0136820>

439 Lange BM, Ahkami A, Markus Lange B, Ahkami A (2013) Metabolic engineering of plant  
440 monoterpenes, sesquiterpenes and diterpenes-current status and future opportunities.  
441 *Plant Biotechnol J* 11:169–96. <https://doi.org/10.1111/pbi.12022>

442 Laterre R, Pottier M, Remacle C, Boutry M (2017) Photosynthetic Trichomes Contain a  
443 Specific Rubisco with a Modified pH-Dependent Activity. *Plant Physiol* 173:2110–2120.  
444 <https://doi.org/10.1104/pp.17.00062>

445 Livak KJ, Schmittgen TD (2001) Analysis of relative gene expression data using real-time  
446 quantitative PCR and the 2- $\Delta\Delta$ CT method. *Methods* 25:402–408.  
447 <https://doi.org/10.1006/meth.2001.1262>

448 Lu Y, Xie L, Chen J (2012) A novel procedure for absolute real-time quantification of gene  
449 expression patterns. *Plant Methods* 8:1–11. <https://doi.org/10.1186/1746-4811-8-9>

450 Maliga P, Sz-Breznovits A, Márton L (1973) Streptomycin-resistant plants from callus culture  
451 of haploid tobacco. *Nat New Biol* 244:29–30

452 Marienhagen J, Bott M (2013) Metabolic engineering of microorganisms for the synthesis of  
453 plant natural products. *J Biotechnol* 163:166–178.  
454 <https://doi.org/10.1016/j.jbiotec.2012.06.001>

455 Moses T, Pollier J (2013) Bioengineering of plant (tri) terpenoids: from metabolic  
456 engineering of plants to synthetic biology in vivo and in vitro. *New Phytol* 200:27–43.  
457 <https://doi.org/10.1111/nph.12325>

458 Navarre C, Sallets A, Gauthy E, et al (2011) Isolation of heat shock-induced *Nicotiana*  
459 *tabacum* transcription promoters and their potential as a tool for plant research and  
460 biotechnology. *Transgenic Res* 20:799–810. <https://doi.org/10.1007/s11248-010-9459-5>

461 Pottier M, Gilis D, Boutry M (2018) The Hidden Face of Rubisco. *Trends Plant Sci* 23:382–  
462 392. <https://doi.org/10.1016/j.tplants.2018.02.006>

463 Sallaud C, Giacalone C, Töpfer R, et al (2012) Characterization of two genes for the  
464 biosynthesis of the labdane diterpene Z-abienol in tobacco (*Nicotiana tabacum*)  
465 glandular trichomes. *Plant J* 72:1–17. <https://doi.org/10.1111/j.1365-313X.2012.05068.x>

466 Saxena B, Subramaniyan M, Malhotra K, et al (2014) Metabolic engineering of chloroplasts  
467 for artemisinic acid biosynthesis and impact on plant growth. *J Biosci* 39:33–41.  
468 <https://doi.org/10.1007/s12038-013-9402-z>

469 Schillmiller AL, Last RL, Pichersky E (2008) Harnessing plant trichome biochemistry for the  
470 production of useful compounds. *Plant J* 54:702–11. <https://doi.org/10.1111/j.1365-313X.2008.03432.x>

472 Van Agtmael MA, Eggelte TA, Van Boxtel CJ (1999) Artemisinin drugs in the treatment of  
473 malaria: From medicinal herb to registered medication. *Trends Pharmacol Sci* 20:199–  
474 205. [https://doi.org/10.1016/S0165-6147\(99\)01302-4](https://doi.org/10.1016/S0165-6147(99)01302-4)

475 van der Fits L, Deakin E, Hoge J, Memelink J (2000) The ternary transformation system:  
476 constitutive virG on a compatible plasmid dramatically increases *Agrobacterium*-  
477 mediated plant transformation. *Plant Mol Biol* 43:495–502

478 van Herpen TWJM, Cankar K, Nogueira M, et al (2010) *Nicotiana benthamiana* as a  
479 production platform for artemisinin precursors. *PLoS One* 5:e14222.  
480 <https://doi.org/10.1371/journal.pone.0014222>

481 Wagner GJ, Wang E, Shepherd RW (2004) New approaches for studying and exploiting an  
482 old protuberance, the plant trichome. *Ann Bot* 93:3–11.  
483 <https://doi.org/10.1093/aob/mch011>

484 Wang B, Kashkooli AB, Sallets A, et al (2016) Transient production of artemisinin in  
485 *Nicotiana benthamiana* is boosted by a specific lipid transfer protein from *A. annua*.  
486 *Metab Eng* 38:159–169. <https://doi.org/10.1016/j.ymben.2016.07.004>

487 Wang E, Gan S, Wagner GJ (2002) Isolation and characterization of the CYP71D16  
488 trichome-specific promoter from *Nicotiana tabacum* L. *J Exp Bot* 53:1891–1897.



489           <https://doi.org/10.1093/jxb/erf054>  
490 Wang E, Wang R, DeParasis J, et al (2001) Suppression of a P450 hydroxylase gene in plant  
491 trichome glands enhances natural-product-based aphid resistance. *Nat Biotechnol*  
492 19:371–374. <https://doi.org/10.1038/86770>  
493 Yoon JM, Zhao L, Shanks J V (2013) Metabolic Engineering with Plants for a Sustainable  
494 Biobased Economy. *Annu Rev Chem Biomol Eng* 4:211–37.  
495 <https://doi.org/10.1146/annurev-chembioeng-061312-103320>  
496

497 **Figure legends**

498 **Fig. 1** Transcript levels in different organs of *N. tabacum*. Transcript levels were normalized  
499 to the mean of those of *NtATP2* and *NtUBQ* genes. Results are shown as mean  $\pm$  SD of three  
500 to five repeats. Different letters indicate significant differences according to a Kruskal-Wallis  
501 test ( $p < 0.05$ ) followed by a Tukey post hoc test

502 **Fig. 2** Transcript levels in trichomes isolated from *N. tabacum* leaves at different  
503 developmental stages. Transcript levels were normalized to the geometric mean of those of  
504 *NtUBQ*, *NtATP2*, and *NtACTIN* genes. St: leaf developmental stage. Stage I: leaf length  $< 2.5$   
505 cm; stage II: leaf length between 2.5 cm and 6.5 cm; stage III: leaf length between 6.5 cm and  
506 15 cm; stage IV: leaf length  $> 15$  cm. Results are shown as mean  $\pm$  SD of three repeats.  
507 Different letters indicate significant differences according to a Kruskal-Wallis test ( $p < 0.05$ )  
508 followed by a Tukey post hoc test

509 **Fig. 3** Absolute transcript levels at stage III of leaf development in *N. tabacum*. Absolute  
510 transcript levels were determined as indicated in the Material and methods. Results are shown  
511 as mean  $\pm$  SD of three repeats. Different letters indicate significant differences according to a  
512 Kruskal-Wallis test ( $p < 0.05$ ) followed by a Tukey post hoc test

513

514 **Fig. 4** Molecular constructs used to generate transgenic *N. tabacum* expressing the  
515 *GUSVENUS* reporter gene under the control of trichome-specific promoters. The transcription  
516 promoter regions of *NtRbcS-T1* (MG493459.1), *NtMALD1* (MG493458.1), *NsCBTS2 $\alpha$*   
517 (HM241151.1), *NtLTPI* (AB625593.1), *NtCYP71D16* (AF166332.1), and *NtCPS2*  
518 (HE588139.1) were amplified and cloned as described in the Material and methods

519

520 **Fig. 5** GUS-VENUS activity in leaves and stems of *N. tabacum* transgenic lines. Venus  
521 detection by confocal imaging and GUS staining were performed on transgenic lines  
522 expressing *GUS-VENUS* under the control of the promoter region of *NtMALD1* (**a-c**),  
523 *NtRbcS-T1* (**d-f**), *NsCBTS2 $\alpha$*  (**g-i**), *CPS2* (**j-l**, white arrowheads point to the labelling of short  
524 glandular trichomes), *NtCYP71D16* (**m-o**), and *NtLTPI* (**p-r**). Left panels: 3D reconstruction  
525 of leaf tissue expressing the VENUS reporter as detected by confocal microscopy. Green:  
526 VENUS signal, magenta: chlorophyll autofluorescence. Middle panels: GUS staining in leaf  
527 cross-sections. Right panels: GUS staining in stem cross-sections. Scale bars: 200  $\mu$ m

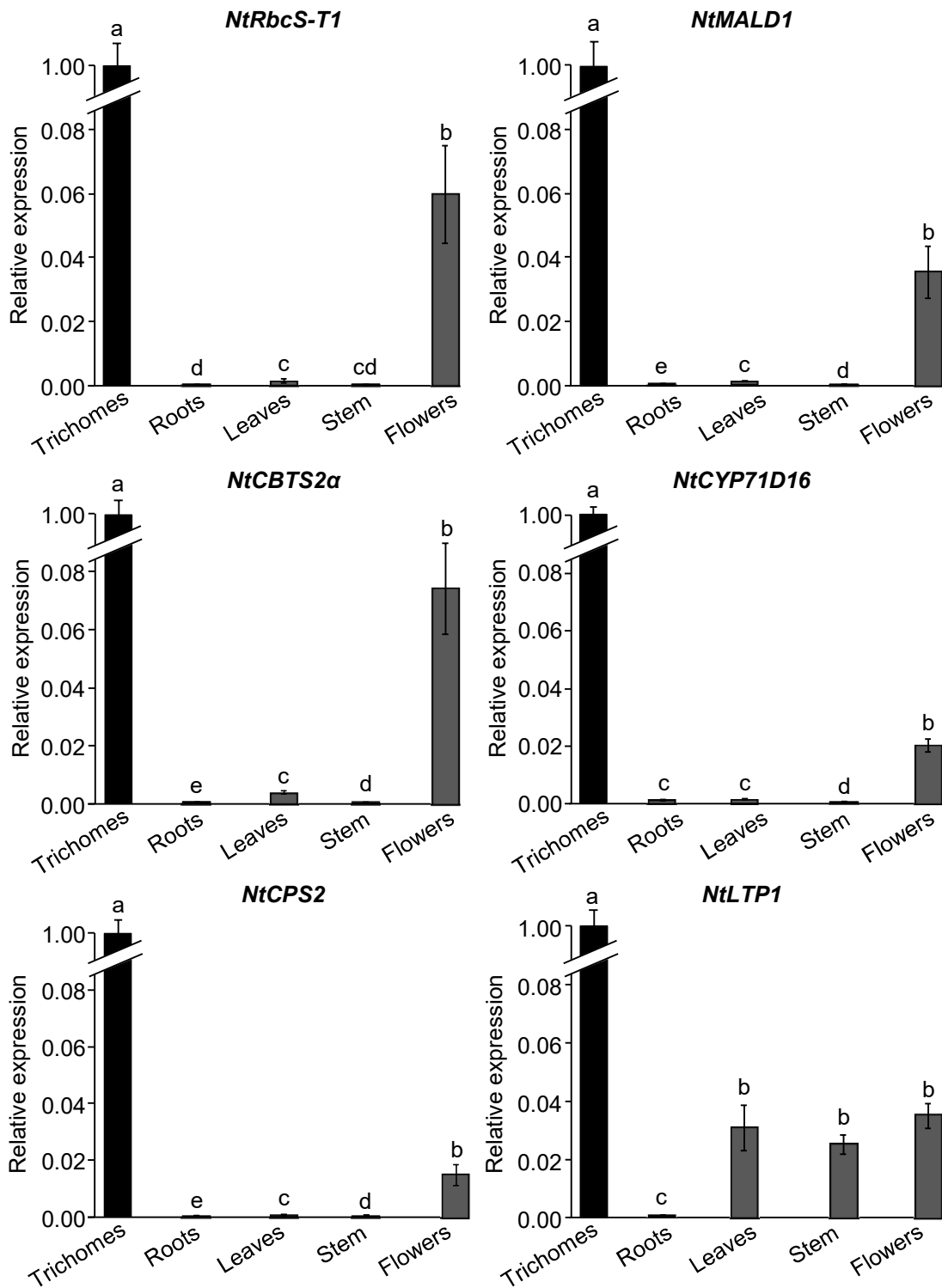


**Fig. 1** Transcript levels in different organs of *N. tabacum*. Transcript levels were normalized to the geometric mean of those of *NtATP2*, *NtUBQ*, and *NtEF1α* genes. Results are shown as mean  $\pm$  SD of three to five repeats. Different letters indicate significant differences according to a Kruskal-Wallis test ( $p < 0.05$ ) followed by a Tukey post hoc test

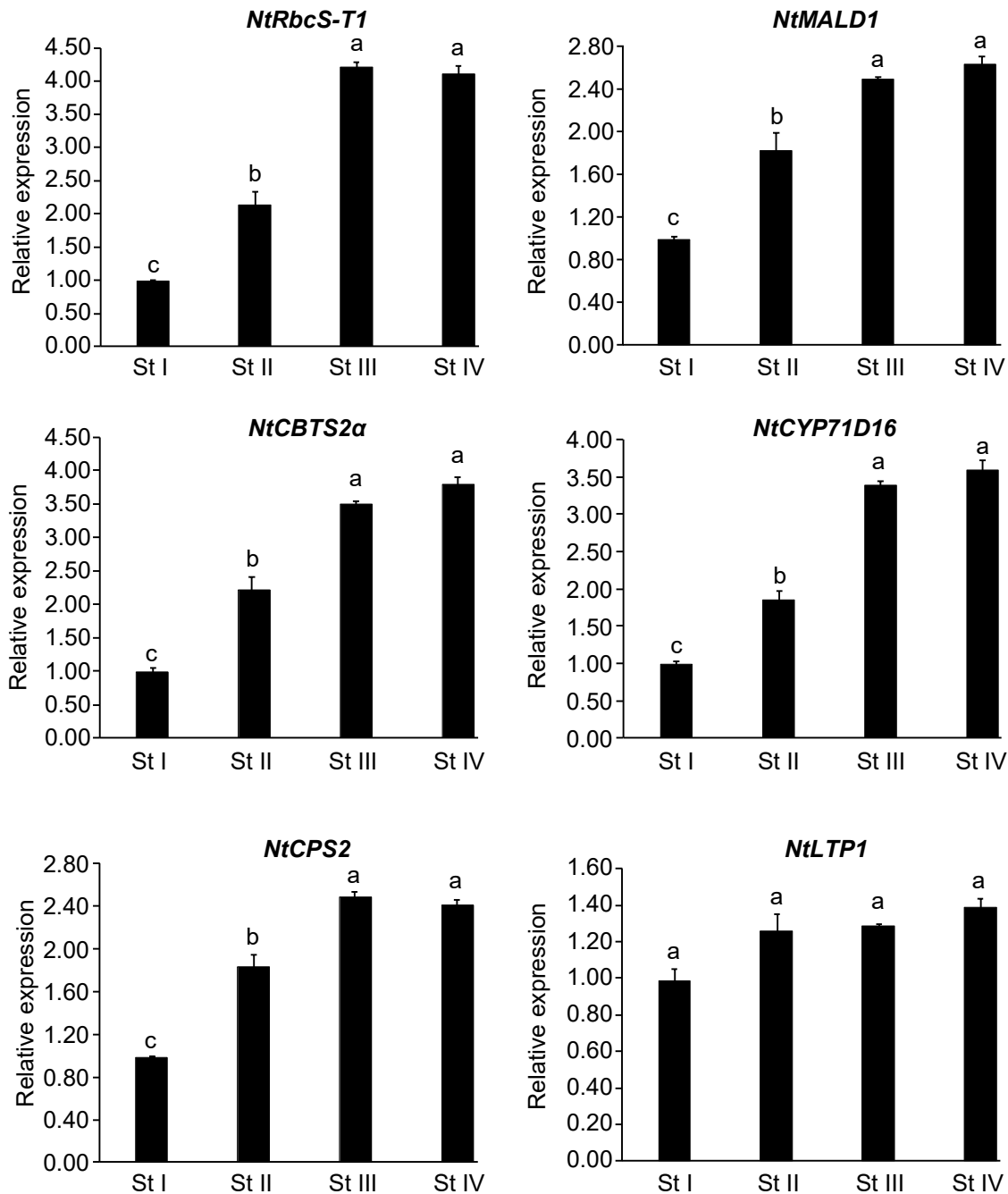


**Fig. 2** Transcript levels in trichomes isolated from *N. tabacum* leaves at different developmental stages. Transcript levels were normalized to the geometric mean of those of *NtUBQ*, *NtATP2*, and *NtACTIN* genes. St: leaf developmental stage. Stage 1: leaf length < 2.5 cm; stage II: leaf length between 2.5 cm and 6.5 cm; stage III: leaf length between 6.5 cm and 15 cm; stage IV: leaf length > 15 cm. Results are shown as mean  $\pm$  SD of three repeats. Different letters indicate significant differences according to a Kruskal-Wallis test ( $p < 0.05$ ) followed by a Tukey post hoc test

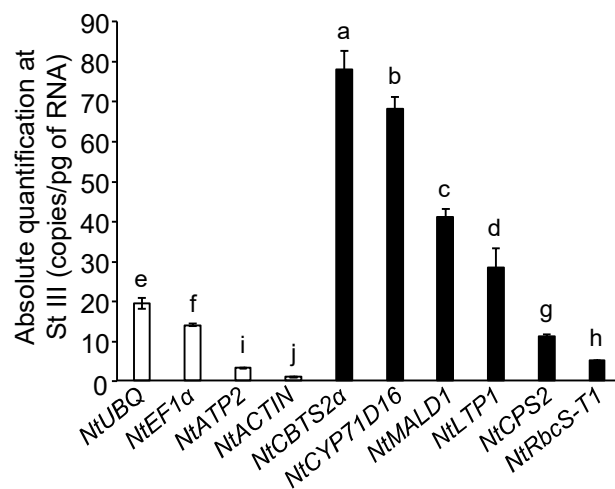


**Fig. 3** Absolute transcript levels at stage III of leaf development in *N. tabacum*. Absolute transcript levels were determined as indicated in the Materials and methods. Results are shown as mean  $\pm$  SD of three repeats. Different letters indicate significant differences according to a Kruskal-Wallis test ( $p < 0.05$ ) followed by a Tukey post hoc test

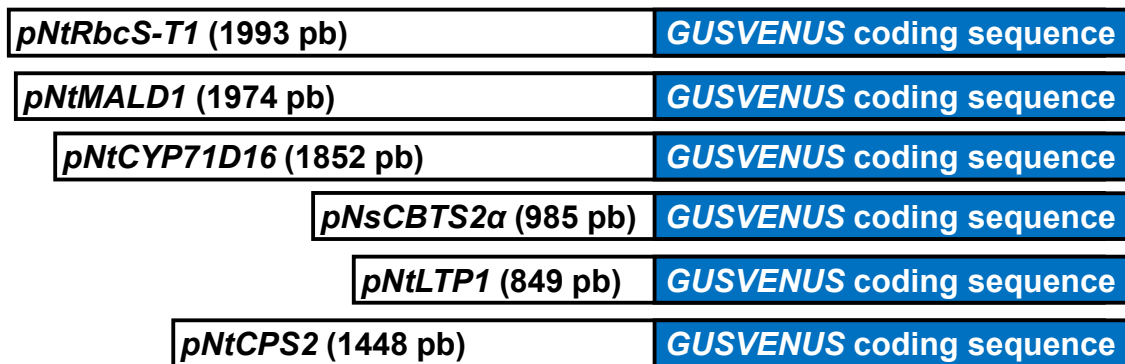


**Fig. 4** Molecular constructs used to generate transgenic *N. tabacum* expressing the *GUSVENUS* reporter gene under the control of trichome-specific promoters. The transcription promoter regions of *NtRbcS-T1* (MG493459.1), *NtMALD1* (MG493458.1), *NsCBTS2α* (HM241151.1), *NtLTP1* (AB625593.1), *NtCYP71D16* (AF166332.1), and *NtCPS2* (HE588139.1) were amplified and cloned as described in the Materials and methods

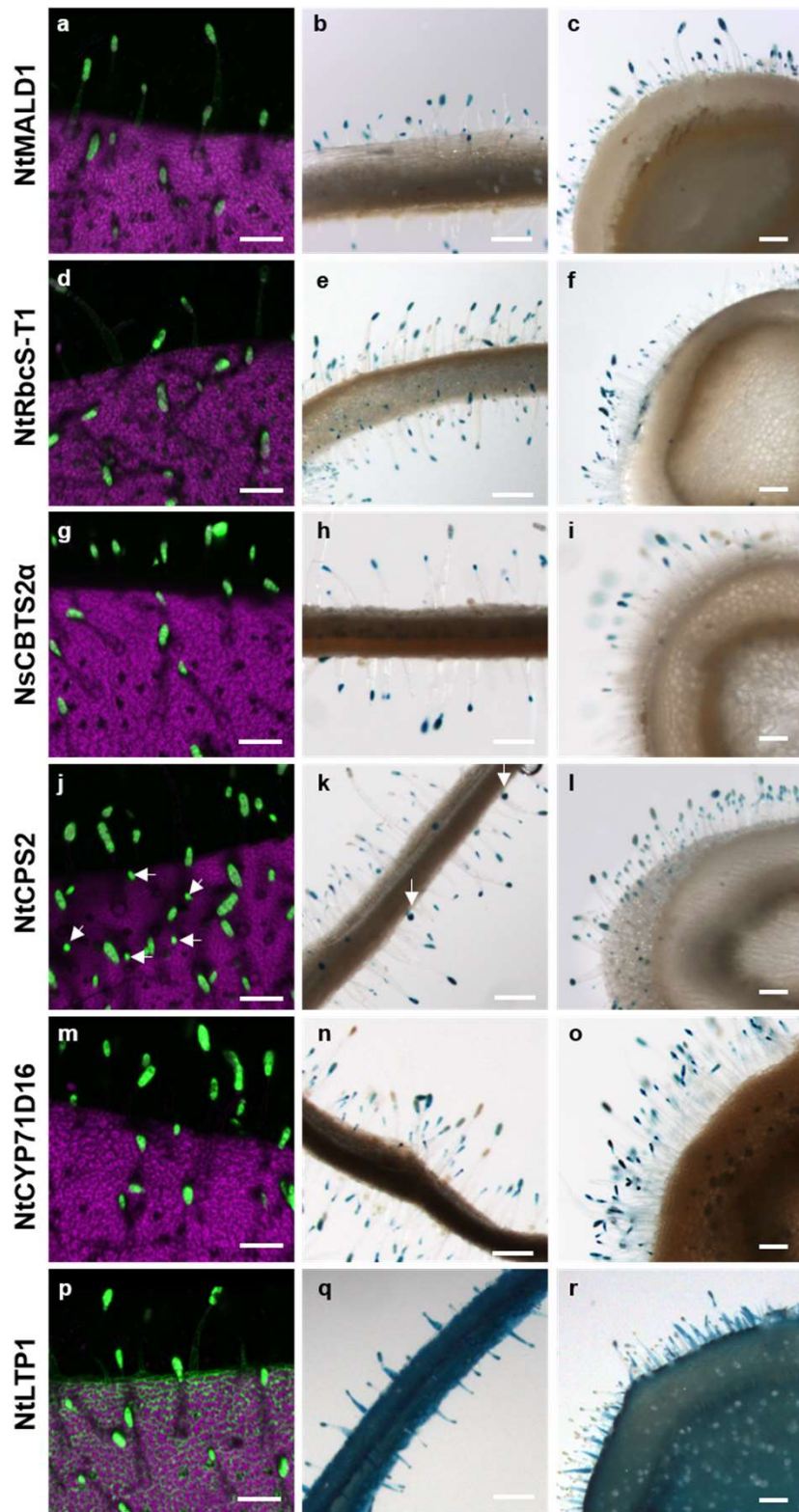


**Fig. 5** GUS-VENUS activity in leaves and stems of *N. tabacum* transgenic lines. Venus detection by confocal imaging and GUS staining were performed on transgenic lines expressing *GUS-VENUS* under the control of the promoter region of *NtMALD1* (a-c), *NtRbcS-T1* (d-f), *NsCBTS2 $\alpha$*  (g-i), *NtCPS2* (j-l, white arrowheads point to the labelling of short glandular trichomes), *NtCYP71D16* (m-o), and *NtLTP1* (p-r, not trichome-specific). Left panels: 3D reconstruction of leaf tissue expressing the VENUS reporter as detected by confocal microscopy. Green: VENUS signal, magenta: chlorophyll autofluorescence. Middle panels: GUS staining in leaf cross-sections. Right panels: GUS staining in stem cross-sections. Scale bars: 200  $\mu$ m